[1]S. L. Glashow, J. Iliopoulos, and L. Maiani, Phys. Rev. D 2, 1285 (1970).
[2]J. P. Berge *et al.*, to be published.
[3]C. H. Albright, to be published.
[4]S. J. Barish *et al.*, Phys. Rev. Lett. 33, 1446 (1974).
[5]J. Ballam *et al.*, Phys. Lett. 56B, 193 (1975).
[6]J. Ballam *et al.*, Phys. Rev. D 5, 545 (1972); H. H. Bingham *et al.*, Phys. Rev. D 8, 1277 (1973).
[7]E. G. Cazzoli *et al.*, Phys. Rev. Lett. 34, 1125 (1975).

Charge Distribution of ^{208}Pb and the Difference in $\rho(r)$ for Pb and Tl Investigated by by Elastic Electron Scattering

H. Euteneuer, J. Friedrich, and N. Voegler
Institut für Kernphysik der Johannes Gutenberg Universität, 65 Mainz, Federal Republic of Germany
(Received 29 September 1975)

Elastic electron-scattering cross sections from ^{208}Pb have been measured for 0.5 fm^{-1} $<q<$ 2.24 fm^{-1}. The charge distribution for this nucleus is determined by a "model-independent" method; it exhibits a bump in the center of the nucleus which is also a characteristic feature of Hartree-Fock calculations. The influence of the 3*s* protons on $\rho(r)$ has been investigated by a difference measurement between lead and thallium isotones.

As a characteristic result of previous electron-scattering experiments on ^{208}Pb the extracted charge distribution exhibited a depression in the center of the nucleus.[1-3] In the following years it was not possible to reproduce this central dip with Hartree-Fock (HF) calculations.[4-6] On the contrary, all calculations yield a central bump, which is mainly due to the 3*s* protons. More recent model-independent evaluations[7,8] of the data from Ref. 2 demonstrated that the cross sections are compatible with a bump, but there remained a discrepancy with HF calculations as well as with muonic data.[12] Because of the importance of this problem the measurement has been repeated with the Mainz electron-scattering facility. In order to get some additional information on the contribution of the last single nucleons (in particular the 3*s* protons), we also measured cross-section ratios between ^{208}Pb and the neighboring nuclei ^{203,205}Tl, ^{204,206,207}Pb, and ^{209}Bi.

The scattering facility has been described in detail by Ehrenberg *et al.*,[9] and therefore only the data of this experiment are given here. The measurements were performed with incident energies of 119.7, 199.5, and 289.0 MeV in a q range from 0.5 to 2.24 fm^{-1}. The heavy nuclei have been measured "simultaneously" with a fast target-exchange equipment; thus errors due to drifts in the scattering apparatus should cancel. The absolute cross-section values have been measured relative to ^{12}C, where the reference carbon cross sections were computed with a charge distribution determined recently in Mainz from new absolute measurements.[10] Many of the points were reproduced several times. In addition to the error from counting statistics we estimated an uncertainty of ± 0.5% for the cross-section ratios and of ± 0.8% for the cross sections relative to carbon. This uncertainty was added quadratically to the statistical error.

The evaluation of the data has been done with the Fourier-Bessel (FB) method described in detail in Ref. 7. The charge distribution is represented by the series

$$\rho_{FB}(r)=\begin{cases}\sum_{1}^{N} a_\nu j_0(q_\nu r), & r\leq R,\\ 0, & r>R,\end{cases} \tag{1}$$

where the values q_ν are given by $\pi\nu/R$ and the coefficients a_ν are related to the Fourier-Bessel transform $F(q_\nu)$ of $\rho(r)$ (i.e., to the form factor if the Born approximation were valid) by

$$a_\nu = F(q_\nu)/2\pi R^3 j_1^2(q_\nu R). \tag{2}$$

[Here $\rho(r)$ is normalized such that $4\pi\int\rho(r)r^2\,dr = 1$.] In practice the coefficients a_ν are fitted to the cross sections by a phase-shift code.[11] In the large-q region, where they are not determined by measurement, the range of possible values is limited by the estimate

$$|F(q_\nu)| \leq c q_\nu^{-4} F_p(q_\nu) \tag{3}$$

(F_p is the proton form factor). The constant c is matched to the last measured cross-section maximum. The error in $\rho(r)$ results from the error

in the measured cross sections (statistical error) and from the lack of knowledge about their large-q behavior (model error).

A fit of the total set of our ^{208}Pb data with a three-parameter Fermi distribution ($n=2$) yields $\chi_{min}^2 = 101.1$ for 28 measured cross-section values; i.e., this analytical form is not compatible with the measurement. However, the data for $q \leq 1.5$ fm^{-1} can be fitted with this distribution ($\chi_{min}^2 = 24.3$ for twenty data points). The parameter w is found to be positive [$w = 0.232(32)$], corresponding to a central depression in $\rho(r)$. In this model-dependent analysis the rms radius is found to be 5.500(24) fm. The resulting distribution is shown in Fig. 1 as a solid line. But the values of w and $\langle r^2\rangle^{1/2}$ and in particular that of χ_{min}^2 increase rapidly if measured cross sections for larger q are included in the analysis.

A fit of our total data set with the much more flexible Fourier-Bessel distribution $\rho_{FB}(r)$ ($\nu = 1$–17, $R = 12.0$ fm) yields a χ_{min}^2 of 13.9. In addition we also took into account the Stanford cross sections[12] with $2.35 < q < 2.73$ fm^{-1}. Because of possible uncertainties in normalization[12] we added an error of ± 4% to the uncertainties of these data. These cross sections do not change the charge distribution which we determined from our data alone, but they reduce the error, mainly for $r < 1$ fm, where it was dominated by the model error (cf. Fig. 2). The values of a_ν for $q_\nu > 2.74$ fm^{-1} have been determined within the restriction of Eq. (3).

The resulting charge distribution with its error band (± 1 standard deviation) is shown in Fig. 1. The statistical and the model errors are also given separately. In addition we show the influence of systematic uncertainties in normalization (± 1%), scattering angle (± 0.03°) and energy (± 0.1%) on $\rho(r)$. Note that not every charge distribution within the error band fits the data because of correlations[7] (for example by normalization). By the analysis of our data with a flexible distribution we find that there exists an increase in $\rho(r)$ for $r < 2$ fm. This feature cannot be reproduced by a Fermi distribution once the sign of w is fixed in the region near the edge of the nucleus. One of the main discrepancies between the measured distribution and the results from HF calculations, which all yield a bump in the center of the nucleus, is now removed. In addition, our $\rho(r)$ is higher in the flat part than that resulting from the Stanford cross sections (cf. Fig. 2), thus the former discrepancy between e^- data and a combined analysis with muonic x rays (Fig. 12 in Ref. 8) seems to be removed. The dashed line in Fig. 1 shows the force-I distribution calculated by Vauthérin and Brink.[5] There remain discrepancies at the edge of the nucleus, and the theoretical rms radius is only 5.44 fm compared with our experimental value of 5.494(24) fm, where the error contains the systematic uncertainties mentioned above.

The results from different experiments are represented most conveniently by the Fourier-

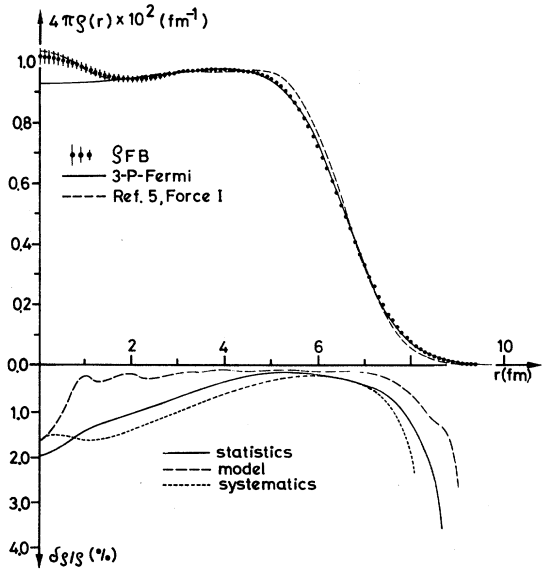

FIG. 1. The charge distribution of ^{208}Pb. The Fourier-Bessel distribution results from the Mainz data and ten Stanford cross sections. The two contributions to the error band (statistical and model error) and the influence of systematic uncertainties of the data on $\rho(r)$ are also given separately.

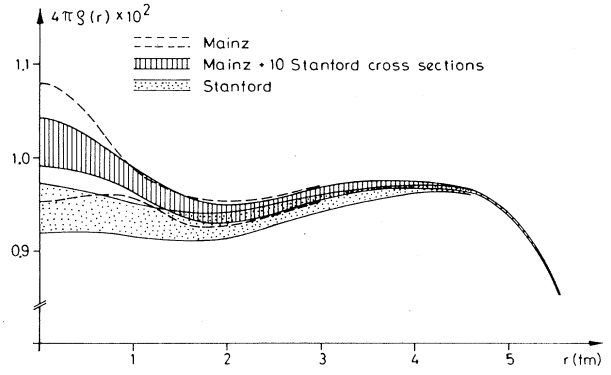

FIG. 2. The inner part of the charge distribution of ^{208}Pb determined from three data sets (Mainz, present experiment; Stanford, Ref. 12).

TABLE I. Fourier-Bessel coefficients of ^{208}Pb. The values below the dashed lines are determined under the restriction of Eq. (3). The errors of the measured a_ν result from counting statistics and an additional error of ±0.8% and ±2.0% (Ref. 11) for the Mainz and Stanford data, respectively. In the combined data set we assumed a normalization uncertainty of ±4% for the ten Stanford cross sections. The numbers in brackets indicate powers of 10.

		Mainz	Stanford	Mainz + ten Stanford cross-sections
ν	qν	aν ± Δaν	aν ± Δaν	aν ± Δaν
1	0.262	0.6341 ± 0.0006 (-3)	0.6338 ± 0.0010 (-3)	0.6341 ± 0.0006 (-3)
2	0.524	0.6229 ± 0.0046 (-3)	0.6178 ± 0.0063 (-3)	0.6236 ± 0.0045 (-3)
3	0.785	-0.4804 ± 0.0055 (-3)	-0.4924 ± 0.0064 (-3)	-0.4794 ± 0.0053 (-3)
4	1.047	-0.3416 ± 0.0028 (-3)	-0.3491 ± 0.0047 (-3)	-0.3419 ± 0.0027 (-3)
5	1.309	0.3526 ± 0.0017 (-3)	0.3568 ± 0.0026 (-3)	0.3528 ± 0.0017 (-3)
6	1.571	0.1206 ± 0.0028 (-3)	0.1252 ± 0.0023 (-3)	0.1201 ± 0.0027 (-3)
7	1.833	-0.1725 ± 0.0039 (-3)	-0.1922 ± 0.0013 (-3)	-0.1726 ± 0.0036 (-3)
8	2.094	-0.5603 ± 0.6085 (-5)	-0.2144 ± 0.0179 (-4)	-0.8707 ± 0.5141 (-5)
9	2.356	0.7833 ± 0.0985 (-4)	0.8738 ± 0.0117 (-4)	0.8885 ± 0.0246 (-4)
10	2.618	0.4262 ± 2.452 (-5)	0.8325 ± 0.2085 (-5)	0.1029 ± 0.0345 (-4)
11	2.880	-0.5088 ± 2.190 (-5)	-0.1874 ± 0.0428 (-4)	-0.1870 ± 0.0528 (-4)
12	3.142	0.3043 ± 1.641 (-5)	-0.3764 ± 0.7026 (-5)	0.9708 ± 7.655 (-6)
13	3.403	-0.1690 ± 1.202 (-5)	0.1476 ± 0.5905 (-5)	-0.3552 ± 6.016 (-6)
14	3.665	0.9001 ± 8.654 (-6)	-0.6469 ± 4.372 (-6)	0.1430 ± 4.400 (-6)
15	3.927	-0.4659 ± 6.158 (-6)	0.2797 ± 3.143 (-6)	-0.6036 ± 31.48 (-7)
16	4.189	0.2357 ± 4.337 (-6)	-0.1201 ± 2.220 (-6)	0.2570 ± 22.21 (-7)
17	4.451	-0.1168 ± 3.026 (-6)	0.5118 ± 15.51 (-7)	-0.1100 ± 15.52 (-7)

Bessel coefficients a_ν fitted to the data since these coefficients are scarcely correlated[7] and they can each be remeasured separately by an experiment in the appropriate q range. The values of a_ν extracted from the different data sets are given in the Table I.

Since a satisfactory theoretical calculation of the charge distribution of ^{208}Pb is missing till now, we have also extracted more detailed information about $\rho(r)$ by investigating the contribution of single nucleons, in particular that of the 3s protons, which are responsible for the bump in the HF calculations. This contribution was investigated by a difference measurement of the isotone pairs ^{206}Pb-^{205}Tl and ^{204}Pb-^{203}Tl. The accuracy of such a measurement of neighboring nuclei is better by a factor of 2 than that of a measurement relative to carbon. The $M1$ contributions to the elastic cross sections of the Tl isotopes have been calculated in Born-approximation with oscillator wave functions. Because these corrections are small (they amount to 1–2% of the charge cross sections only at high q), the result should be sufficiently accurate. Possible contributions from the low-lying levels at 279 and 205 keV for ^{203}Tl and ^{205}Tl, respectively, are found to be compatible with zero within an error of 1% of the area of the elastic peak and they show no structure in q reminiscent of a $C2$ transition. They therefore were assumed to be negligible. The measured cross-section ratios $\sigma(^{206}\text{Pb})/\sigma(^{205}\text{Tl})$ are shown in Fig. 3.

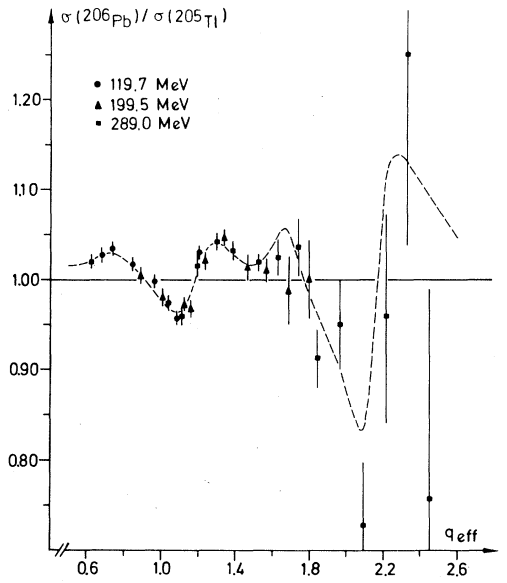

FIG. 3. Measured cross-section ratios of ^{206}Pb and ^{205}Tl and best fit (dashed curve). $q_{\text{eff}} = q(1 + 25.2/E)$.

Again, the evaluation of the cross-section ratios has been done with the Fourier-Bessel method ($\nu = 1$–17, $R = 10.5$ fm); now the ratios beyond

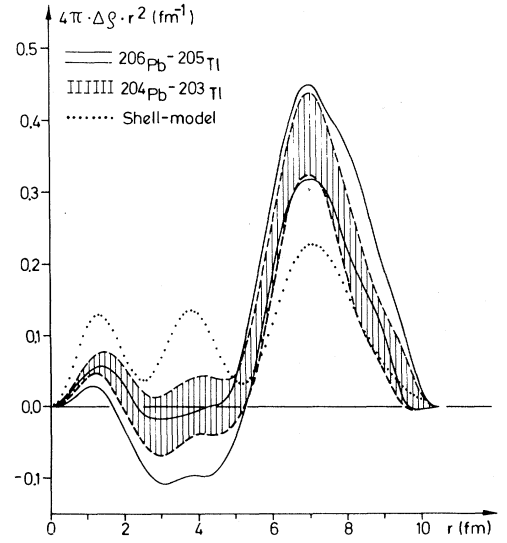

FIG. 4. Differences of the charge distribution of lead and thallium isotopes ($4\pi \int \Delta\, \rho r^2\, dr = 1$).

the measured q range are estimated within the limits given by Eq. (3) for the difference of the form factors (the Fourier transform of the $3s$ harmonic oscillator wave function is well within these limits). The results are shown in Fig. 4. For comparison we also plotted the distribution of a $3s_{1/2}$ shell-model proton ($b_{osc} = 2.54$ fm),[4] where the proton distribution has been folded. If the last proton of the lead nucleus is interpreted as a shell-model proton, it seems to push charge away from the interior of the nucleus. This feature seems not to be affected very much by differences in the neutron configuration as can be seen from the two $\Delta\rho$ bands. Further details and results for the other isotones and isotopes will be presented in another publication.[13]

The results presented in this paper are part of the work of the electron scattering group of Professor Dr. H. Ehrenberg. The authors are very indebted to the entire laboratory staff for rendering these measurements possible. The numerical calculations have been done on the CD 3300 and the TR 440 in the Rechenzentrum der Universität Mainz.

[1]J. B. Bellicard and K. J. van Oostrum, Phys. Rev. Lett. 19, 242 (1967).
[2]J. Heisenberg, R. Hofstadter, J. S. McCarthy, I. Sick, B. C. Clark, R. Herman, and D. G. Ravenhall, Phys. Rev. Lett. 23, 1402 (1969).
[3]J. Friedrich and F. Lenz, Nucl. Phys. A183, 523 (1972).
[4]J. W. Negele, Phys. Rev. C 1, 1260 (1970).
[5]D. Vauthérin and D. M. Brink, Phys. Rev. C 5, 626 (1972).
[6]A. Faessler, J. E. Galonska, J. W. Ehlers, and S. A. Moszkowski, Nuovo Cimento 11A, 63 (1972).
[7]B. Dreher, J. Friedrich, K. Merle, H. Rothhaas, and G. Lührs, Nucl. Phys. A235, 219 (1974).
[8]J. L. Friar and J. W. Negele, Nucl. Phys. A212, 93 (1973).
[9]H. Ehrenberg, H. Averdung, B. Dreher, G. Fricke, H. Herminghaus, R. Herr, H. Hultzsch, G. Lührs, K. Merle, R. Neuhausen, G. Nöldeke, H. M. Stolz, V. Walther, and H. D. Wohlfahrt, Nucl. Instrum. Methods 105, 253 (1972).
[10]K. Merle, thesis, Universität Mainz, 1975 (unpublished).
[11]B. Dreher, program Dreher 3.
[12]J. Heisenberg, private communication.
[13]H. Euteneuer, thesis, Universität Mainz, 1975 (unpublished).

Multistep Core-Exchange Analysis of $^{16}O + ^{18}O$ Scattering with the Full-Recoil Calculation

B. Imanishi
Institute for Nuclear Study, University of Tokyo, Tanashi, Tokyo, Japan

and

K.-I. Kubo
Department of Physics, University of Tokyo, Hongo, Tokyo, Japan

(Received 6 October 1975)

Multistep core-exchange analysis has been performed for the scattering of $^{16}O + ^{18}O$ at four different incident energies. It has been found that the recoil effects are very important for reproducing the energy dependence of the observed cross sections. The multistep effects due to the core-exchange process are very small.

In $^{16}O + ^{18}O$ elastic scattering at an incident energy above the Coulomb barrier, a strongly oscillating angular distribution and an enhancement of cross section have been observed in the backward angular region.[1-3] These phenomena are interpreted as due to the existence of the core-exchange process.[4] Gelbke *et al.*[1,2] have investigated such a core-exchange process using the approach of a linear combination of nuclear orbitals (LCNO)[4] under the assumption that two neutrons in the $d_{5/2}$ shell of the ^{18}O ground state are transferred as a ^1S dineutron. The angular distributions calculated for three different incident energies, $E_{lab} = 24$, 28, and 32 MeV, show a general fit to the experimental data. However, in order to get a more precise fit in the backward angular region, incident-energy–dependent spectroscopic factors have been required.[1] As the incident energy increases, the backward cross sections calculated from the LCNO using a constant spectroscopic factor increase faster than those observed. Gelbke *et al.*[1] then suggested several reasons for such a result: The assumption of ^1S dineutron transfer may not be adequate or there may exist another strong coupled-channels effect arising from the inelastic $^{18}O^*(2^+, 1.95$ MeV)-